UC Riverside

UC Riverside Previously Published Works

Title

The effect of different fertigation strategies and furrow surface treatments on plant water and nitrogen use

Permalink

https://escholarship.org/uc/item/87x7w7fp

Journal

Irrigation Science, 34(1)

ISSN

0342-7188

Authors

Šimůnek, Jirka
Bristow, Keith L
Helalia, Sarah A
et al.

Publication Date

2016

DOI

10.1007/s00271-015-0487-z

Peer reviewed

eScholarship.org Powered by the California Digital Library
University of California

Irrig Sci (2016) 34:53–69
DOI 10.1007/s00271-015-0487-z

ORIGINAL PAPER

The effect of different fertigation strategies and furrow surface treatments on plant water and nitrogen use

Jirka Šimůnek[1] · Keith L. Bristow[2] · Sarah A. Helalia[1] · Altaf A. Siyal[3]

Received: 12 April 2015 / Accepted: 30 November 2015 / Published online: 21 December 2015
© Springer-Verlag Berlin Heidelberg 2015

Abstract Furrow irrigation and fertigation systems should be designed and managed to optimize the availability of water and fertilizer to plants and minimize their losses through evaporation, deep drainage and leaching. We developed a furrow irrigation submodule for HYDRUS (2D/3D) and used it to evaluate the effects of different furrow soil surface treatments and different timings of fertigation on root water and solute uptake, deep drainage and solute leaching in a loamy soil. Numerical simulations showed that more water was available for transpiration in the treatments with plastic placed at the furrow bottom compared to the control treatments. However, more water was lost due to evaporation and less water was drained from the soil profile for these treatments. The highest and lowest root solute uptake was achieved when fertigation was applied in the middle and at the beginning of the irrigation cycle, respectively. The least amount of solute was leached from the soil profile for treatments with the plastic bottom and when fertigation was applied at the end of the irrigation cycle. The scenarios with plastic and irrigation in alternate furrows showed a reduction in transpiration and yield, more water loss due to deep drainage, and less water lost due to evaporation. However, similar crop yields were obtained for this alternate furrow strategy as for the control furrow surface treatments. When only half the water was used for irrigation in this scenario, the reduction in yield was less than 20 % compared to the control treatments, producing higher water-use efficiency.

Communicated by J. Hornbuckle.

✉ Jirka Šimůnek
Jiri.Simunek@ucr.edu

Keith L. Bristow
Keith.Bristow@csiro.au

Altaf A. Siyal
aasiyal.uspcasw@muet.edu.pk

[1] Department of Environmental Sciences, University of California Riverside, Riverside, CA 92521, USA

[2] CSIRO Agriculture Flagship, PMB Aitkenvale, Townsville, QLD 4814, Australia

[3] U.S.-Pakistan Centers of Advanced Studies in Water, Mehran University of Engineering and Technology, Jamshoro, Pakistan

Introduction

Fertigation can be defined as the injection of various water-soluble chemicals, such as fertilizers or soil amendments, into agricultural irrigation systems, including drip, sprinkler and surface irrigated systems (Sabillón and Merkley 2004). Fertigation is most commonly used with drip and sprinkler systems (e.g., Cote et al. 2003; Hanson et al. 2006), while its use with surface irrigation methods is much less common (Sabillón and Merkley 2004; Soroush et al. 2012; Ebrahimian et al. 2014). Since furrow irrigation is the most frequently used irrigation method internationally, furrow fertigation has great potential to become a cost-effective method of applying fertilizers to agricultural fields (Soroush et al. 2012). To be successful, the furrow irrigation and fertigation systems should be designed and managed so that the application and distribution of water and fertilizer are efficient and uniform, with minimal surface runoff at the lower end of the field, and minimal deep drainage and leaching below the crop root zone (Sabillón and Merkley 2004).

Timing of fertigation during an irrigation cycle, and resulting availability of applied fertilizers to plants, has received considerable attention in the past (e.g., Hou et al.

2007), especially for drip irrigated systems (e.g., Cote et al. 2003; Gärdenäs et al. 2005; Hanson et al. 2006). For example, Cote et al. (2003) used the HYDRUS-2D model (Šimůnek et al. 2008) to evaluate the spatial distribution of a fertilizer, which was applied either at the beginning or at the end of subsurface drip irrigation. They concluded, contrary to general expectations, that for highly permeable coarse-textured soils, nutrients applied at the beginning of an irrigation cycle will reside in larger amounts near to and above the emitter than when applied at the end of an irrigation cycle, thereby making them less susceptible to leaching losses. Gärdenäs et al. (2005) evaluated five different fertigation strategies for three different microirrigation systems. They assumed that fertilizers can be applied in a short pulse either at the beginning, in the middle, or at the end of an irrigation cycle, in the middle half of the irrigation cycle, or continuously. They considered a micro-sprinkler system, subsurface and surface irrigation tapes, and subsurface drip irrigation systems. Gärdenäs et al. (2005) concluded that fertigation applied at the beginning of an irrigation cycle tends to increase seasonal nitrate leaching and that fertigation applied at the end of an irrigation cycle tends to reduce nitrate leaching. While Cote et al. (2003) evaluated only one irrigation cycle, Gärdenäs et al. (2005) simulated a 1-month time period with multiple irrigation cycles, which may explain the different results obtained in these two studies.

There are many studies that evaluated fertigation timing in furrow irrigation (e.g., Bouwer et al. 1990; Playán and Faci 1997; Sabillón and Merkley 2004; Adamsen et al. 2005; Burguete et al. 2009; Ebrahimian et al. 2013b). For example, Bouwer et al. (1990) and Soroush et al. (2012) recommended that in order to avoid leaching of fertilizers to groundwater, fertigation should be applied toward the end of an irrigation event. Playán and Faci (1997), however, concluded that applying fertilizer at a constant rate during the entire irrigation event is usually the best solution, since an instantaneous release of fertilizer into the irrigation stream often produces low fertilizer uniformities in the field. Sabillón and Merkley (2004) reported that timing of fertigation is significantly affected by soil infiltration characteristics, furrow length and slope.

Adamsen et al. (2005) carried out field experiments to compare different strategies for timing injection of bromide, as a surrogate for nitrate, into the irrigation water during border irrigation. The bromide was injected either during the first half, the middle half, or the last half of the irrigation, or during the entire irrigation. Adamsen et al. (2005) concluded, similarly to Playán and Faci (1997) and Abbasi et al. (2003c), that the best distribution uniformity is obtained when bromide was injected during the entire irrigation event. Burguete et al. (2009) developed a simulation model, which considered overland water flow, solute transport and infiltration, and used it to evaluate the effects of irrigation discharge, fertilizer application timing and furrow geometry on fertilizer uniformity. Ebrahimian et al. (2013b) used genetic algorithms and the one-dimensional surface and two-dimensional subsurface models to optimize timing of fertigation in alternate furrow irrigation. They concluded that by optimizing the start time and the duration of fertilizer injection, they could reduce nitrate losses due to deep percolation and surface runoff by up to 50 %.

In standard irrigation furrows, water infiltration into the soil profile is driven by gravitational forces in the downward vertical direction and by capillary forces horizontally and upward into the ridge. In furrows, in which vertically downward infiltration from the bottom of the furrow is either reduced or eliminated altogether (Siyal et al. 2012), water infiltration is driven mainly by capillary forces horizontally and upward into the ridge. The recommendations for fertigation timing, some of which appear contradictory even for standard furrows (e.g., Soroush et al. 2012; Playán and Faci 1997), may thus be different for these non-conventional furrows (with reduced downward infiltration) and may resemble drip irrigation systems, in which capillary forces play an important role.

The HYDRUS (2D/3D) model and its predecessors, such as SWMS-2D and HYDRUS-2D, have been widely used in the past to simulate water flow and/or solute transport for furrow irrigation systems (e.g., Benjamin et al. 1994; Abbasi et al. 2003a, b, 2004; Rocha et al. 2006; Wöhling et al. 2004a, b, 2006; Mailhol et al. 2007; Warrick et al. 2007; Wöhling and Schmitz 2007; Wöhling and Mailhol 2007; Crevoisier et al. 2008; Lazarovitch et al. 2009; Ebrahimian et al. 2012, 2013a, b; Zerihun et al. 2014). For example, Benjamin et al. (1994) simulated fertilizer distribution in the soil under broadcast fertilization for conventional and alternate furrow irrigation. They concluded that fertilizer applied on the non-irrigated furrows may not be taken up by plants because of the low water content in the upper layer of this furrow. Rocha et al. (2006) carried out an extensive sensitivity analysis to investigate the effects of various soil hydraulic properties on subsurface water flow below furrows. Abbasi et al. (2003a, b, 2004) obtained satisfactory agreement between measured and predicted soil water contents and solute concentrations along the blocked-end furrow cross-section using the HYDRUS-2D model. Similarly, Mailhol et al. (2007) and Crevoisier et al. (2008) found that the HYDRUS-2D model performed well in simulating soil matric potential, nitrate concentrations and nitrogen leaching in conventional and alternate furrow irrigated systems in season-long studies, which included both root water and nutrient uptake.

Wöhling and Schmitz (2007) developed a numerical model that coupled 1D surface flow (zero-inertia),

HYDRUS-2D, and a crop growth model. This model was then used to adequately predict advance and recession times, soil moisture and crop yield (Wöhling and Mailhol 2007). Ebrahimian et al. (2012) compared the performance of the HYDRUS-1D and HYDRUS-2D simulation models to simulate water flow and nitrate transport for conventional furrow irrigation, fixed alternate furrow irrigation, and variable alternate furrow irrigation using different fertigation strategies. Ebrahimian et al. (2013a, b) used the one-dimensional surface and two-dimensional subsurface models to minimize nitrate losses in two types of alternate furrow fertigation systems.

While some of these studies involved only simulations (e.g., Rocha et al. 2006; Warrick et al. 2007; Lazarovitch et al. 2009), in many studies the HYDRUS (2D/3D) model was calibrated and tested using experimental data (e.g., Abbasi et al. 2003a, b, 2004; Wöhling and Mailhol 2007; Crevoisier et al. 2008; Zerihun et al. 2014), providing its future users with confidence that the model can adequately describe these complex systems. However, very few of these studies, with the exception of Gärdenäs et al. (2005) and Wöhling and Schmitz (2007), considered multiple irrigation/fertigation cycles and the effects of plants on subsurface flow and transport processes. Most studies evaluated only a single irrigation cycle and neglected the effects of plant roots on subsurface processes.

While many of the studies discussed above focused on flow and transport along a furrow, Abbasi et al. (2003a, b) and Siyal et al. (2012) evaluated subsurface flow and transport in the soil profile perpendicular to the furrow. Siyal et al. (2012) developed a furrow irrigation submodel for HYDRUS (2D/3D) and then used this model to analyze the effects of different furrow irrigation rates, different treatments of the soil surface at the bottom of the furrow, and different initial locations of the fertilizer on water and solute leaching in a furrow irrigated system. Siyal et al. (2012) did not, however, apply fertilizers with the irrigation water nor did they consider root water uptake. On the contrary, they assumed that the fertilizer (nitrogen) was initially located at five different locations, ranging from the bottom of the furrow to the top of the ridge, and allowed the solute to move with the water without being intercepted by plant roots. The different soil treatments at the bottom of the furrow included (a) untreated (S_o), i.e., it remained as a control with normal soil hydraulic properties, (b) compacted (S_c), with its hydraulic conductivity reduced by 80 % of S_o, and (c) covered with an impermeable polymer membrane (S_p) with zero conductivity.

The objectives of this study are (a) to extend the furrow irrigation submodel of Siyal et al. (2012) to include processes of precipitation, evaporation and fertigation in the furrow, (b) to evaluate this model with respect to different water and solute fluxes and volumes, and corresponding solute concentrations, in the furrow, as well as in the soil profile, (c) to evaluate the effectiveness of different treatments of the furrow bottom and fertigation timing strategies to supply water and nutrients to plants, and (d) to evaluate the combined effects of plant water and nutrient uptake with different furrow treatments and fertigation strategies to limit water and nutrient leaching and to provide optimal conditions for plants. Rather than evaluating only a single irrigation/fertigation cycle, which may not fully address the long-term processes such as root water and nutrient uptake and leaching, the objective of this study is to evaluate cumulative effects of a series of irrigation/fertigation cycles.

Materials and methods

Numerical simulations of the furrow irrigation system were carried out with the HYDRUS (2D/3D) software package (Šimůnek et al. 2008), which was updated with the modified furrow mass balance submodule (Siyal et al. 2012). Below, we first describe the additional modifications incorporated into the furrow mass balance submodule of Siyal et al. (2012) and follow with a brief description of the HYDRUS (2D/3D) software.

The furrow mass balance module

Siyal et al. (2012) developed a furrow irrigation module, which calculated the water level in the furrow based on the mass balance in the furrow for a specified irrigation flux, Q_p, and calculated infiltration flux, Q_{in}. The infiltration flux was calculated using the HYDRUS (2D/3D) software, which adjusts boundary conditions at the bottom and sides of the furrow in response to changes in the water level in the furrow (Fig. 1).

In addition to the irrigation and infiltration processes considered by Siyal et al. (2012), in this study we also account for precipitation, evaporation and fertigation. The mass balance equation for water in the furrow is expressed as:

$$\frac{dS}{dt} = Q_p(t) - Q_{in}(t) + (P - E)b \quad (1)$$

where S is the volume of water in the half-furrow [L^2], Q_p and Q_{in} are irrigation and infiltration fluxes to/from the half-furrow [L^2T^{-1}], respectively, P and E are precipitation and evaporation rates [LT^{-1}], respectively, and b is the half-width of the water surface in the furrow [L]. The height of the water level in the furrow, h_w [L], is calculated in the same ways as in Siyal et al. (2012) except that we now also include the last term of (1) to account for precipitation and evaporation.

The module requires as input the description of the geometry of the furrow (α and a), the supply rate (Q_p),

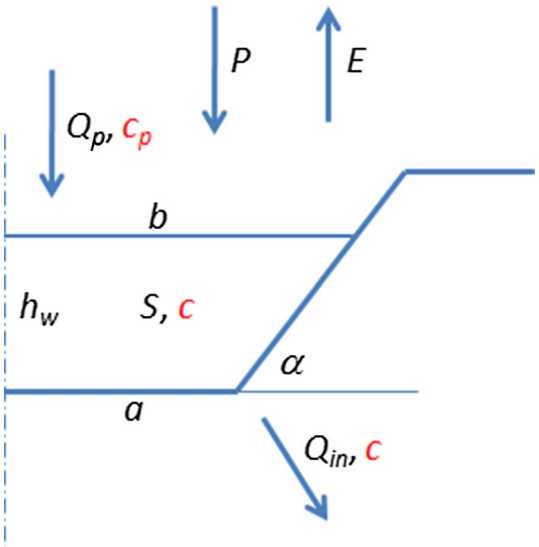

Fig. 1 Schematic showing a half-furrow and the implementation of a special boundary condition accounting for variable water depth in the furrow (Q_p is the irrigation water supply rate, c_p is the solute concentration in the incoming irrigation water, Q_{in} is the water infiltration rate from the furrow into the soil profile across the furrow walls, c is the solute concentration in the furrow water and in the infiltration water, S is the volume of water in the half-furrow, h_w is the water level in the furrow, α is the angle defining the slope of the ridge side, a is the half-width of the bottom of the furrow, b is the half-width of the water surface, and P and E are precipitation and evaporation fluxes, respectively)

precipitation and evaporation fluxes (P and E), and then either the duration of irrigation or the maximum water level ($h_{w,max}$) that can be reached before water supply is stopped. The module calculates the position of the water level in the furrow by considering the irrigation flux, which is the result of the numerical solution of the Richards equation for specified dynamic boundary conditions. The relevant parts of the boundary below and above the water level in the furrow are in HYDRUS assigned the time-variable pressure head (Dirichlet) and seepage face boundary conditions, respectively. HYDRUS calculates which part of the seepage face boundary is active (with a prescribed zero pressure head) and which is inactive (with a prescribed zero flux or atmospheric boundary conditions). Once the furrow is empty of water, the atmospheric BC is applied at the furrow bottom in addition to the sides of the ridge (Siyal et al. 2012).

The mass balance equation for solute in the furrow is expressed as:

$$\begin{aligned}\frac{\mathrm{d}(Sc)}{\mathrm{d}t} &= S\frac{\mathrm{d}c}{\mathrm{d}t} + c\frac{\mathrm{d}S}{\mathrm{d}t} = Q_\mathrm{p}(t)c_\mathrm{p} - Q_\mathrm{in}(t)c \\ S\frac{\mathrm{d}c}{\mathrm{d}t} &= Q_\mathrm{p}(t)c_\mathrm{p} - Q_\mathrm{in}(t)c - c\left[Q_\mathrm{p}(t) - Q_\mathrm{in}(t) + (P-E)b\right] \\ S\frac{\mathrm{d}c}{\mathrm{d}t} &= Q_\mathrm{p}(t)\left(c_\mathrm{p} - c\right) - c[(P-E)b] \end{aligned} \quad (2)$$

where c_p is the solute concentration of irrigation water (fertigation) [ML^{-3}; or dimensionless], and c is the average solute concentration of the furrow water and hence the concentration of the infiltrating water [ML^{-3}]. Note that we assume that precipitation and evaporation fluxes are devoid of solutes and that there is an instantaneous and complete mixing of solute in the furrow. Precipitation will therefore lead to dilution of solute in the furrow water, while evaporation will lead to increasing concentrations. The module requires as input the solute concentration in the irrigation water (c_p) and the timing of fertigation (i.e., the beginning and the end time of fertigation). The module then calculates the solute concentration in the furrow water, c, which is subsequently used in a Cauchy (concentration flux) boundary condition together with the local infiltration flux calculated by HYDRUS.

Governing water flow and solute transport equations

Variably-saturated water flow in soil is described in HYDRUS by the modified Richards equation:

$$\frac{\partial\theta}{\partial t} = \frac{\partial}{\partial x_i}\left[K\left(K_{ij}^A\frac{\partial h}{\partial x_j} + K_{iz}^A\right)\right] - S \quad (3)$$

where θ is the volumetric water content [L^3L^{-3}], h is the pressure head [L], S is a sink term accounting for root water uptake [T^{-1}], x_i ($i = 1,2$) are spatial coordinates [L], t is time [T], K_{ij}^A are components of a dimensionless anisotropy tensor $\mathbf{K}^A$, and K is the unsaturated hydraulic conductivity function [LT^{-1}] given as the product of the relative hydraulic conductivity K_r and the saturated hydraulic conductivity K_s [LT^{-1}].

The soil hydraulic parameters for loam [the same soil as used by Siyal et al. (2012)] were taken from the soil catalog provided by the HYDRUS software. The values of these parameters are: residual water content = 0.078; saturated water content = 0.43; shape parameters α and n are 0.036 cm^{-1} and 1.56, respectively; saturated hydraulic conductivity = 24.96 cm/day. For this soil, the field capacity is 0.165 (pressure head −330 cm) and the water content at the wilting point (pressure head −15,000 cm) is 0.088 cm^3 cm^{-3}. The critical pressure head and water content values when evaporation falls below its potential value are −10,000 cm and 0.091, respectively.

Solute transport is described in HYDRUS by the convection–dispersion equation:

$$\frac{\partial\theta c}{\partial t} = \frac{\partial}{\partial x_i}\left(\theta D_{ij}\frac{\partial c}{\partial x_j}\right) - \frac{\partial q_i c}{\partial x_i} - Sc_r \quad (4)$$

where c is the solute concentration [ML^{-3}], q_i is the i th component of the volumetric flux density [LT^{-1}], D_{ij} is the dispersion coefficient tensor [L^2T^{-1}], and c_r is the concentration of the sink term [ML^{-3}]. The longitudinal and

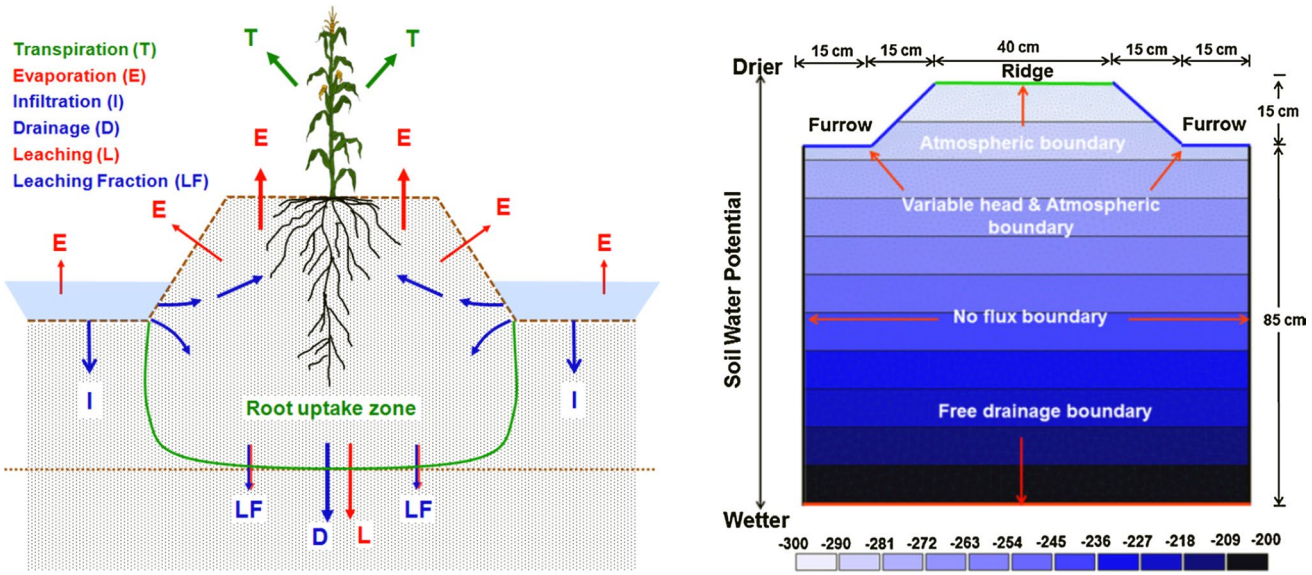

Fig. 2 Schematic representation of the transport domain showing the main hydrological fluxes (*left*) and initial and boundary conditions (*right*; see also Siyal et al. 2012)

transverse dispersivities were set at 10 and 1 cm that is at one-tenth and one-hundreds of the depth of the soil profile (Beven et al. 1993), respectively. Note that no reactions are considered in (4) so it can only be used to describe the transport of nonreactive solutes such as chloride and nitrate.

Root water and nutrient uptake

Root water uptake is described in HYDRUS using the approach of Feddes et al. (1978):

$$S(h) = \alpha(h) b(x,z) L_t T_p \tag{5}$$

where S is the root water uptake rate [T^{-1}], $\alpha(h)$ is a water stress response function, $b(x, z)$ is a normalized function describing the spatial distribution of water uptake [L^{-2}], L_t is the width [L] of the soil surface associated with the transpiration process (L_t = 40 cm; surface of the furrow ridge, see the definition of the transport domain in Fig. 2), and T_p is the potential transpiration rate [LT^{-1}] (T_p = 0.8 cm/day). The following parameters of the stress response function (typical for many crops) were used in our study: $h_1 = -10$ cm, $h_2 = -25$ cm, $h_3 = -200$ cm, and $h_4 = -8000$ cm (Feddes et al. 1978).

The two-dimensional root distribution function $b(x,z)$ of Vrugt et al. (2001, 2002) was used to describe the spatial distribution of roots:

$$b(x,z) = \left(1 - \frac{z}{Z_m}\right)\left(1 - \frac{x}{X_m}\right) e^{-\left(\frac{p_z}{Z_m}|z^*-z| + \frac{p_x}{X_m}|x^*-x|\right)} \tag{6}$$

where X_m and Z_m are the maximum rooting lengths in the x and z directions [L], respectively; x and z are distances from the origin of the plant in the x and z directions [L], respectively; and p_x [-], p_z [-], x^*[L], and z^*[L] are empirical parameters. The plant was centered in the middle of the ridge. The maximum extent of roots in the vertical (Z_m) and horizontal (X_m) directions was set at 60 and 35 cm, respectively, parameters x^* and z^* (sometimes referred to as *Depth and Radius of Maximum Intensity*) were set at 30 and 20 cm, respectively, and parameters p_x and p_z were set at one for $x < x^*$ and $z < z^*$, and zero elsewhere. Note that the spatial distribution of roots was considered to be constant in time, i.e., no root growth was included in the simulations.

Only non-compensated root water uptake and passive root nutrient uptake (Šimůnek and Hopmans 2009) were considered in this study, i.e., c_r in (4) was assumed to be equal to the solute concentration at any particular location. Using this approach allows us to better evaluate the availability of water and solutes to plant roots.

Flow domain, initial and boundary conditions

Figure 2 (left) shows a schematic representation of the transport domain with the main hydrological fluxes. It was assumed that the total incoming energy (ET_p) was equal to 1 cm/day, which corresponds to conditions in January in north Queensland, Australia. This incoming energy was divided at the top of the furrow into potential evaporation (E_p) of 0.2 cm/day and potential transpiration (equivalent to root water uptake) (T_p) of 0.8 cm/day. All incoming energy

(ET_p = 1 cm/day) was assumed to reach the water in the furrow, or the bottom and sides of the furrow. The total potential flux at the soil surface of the transport domain during one irrigation cycle was thus equal to 700 cm^2/week (= 1 cm/day × 100 cm × 7 day/week).

Figure 2 (right) shows the dimensions of the transport domain with two half-furrows and the applied initial and boundary conditions, which were the same as in Siyal et al. (2012). The soil profile was assumed to be initially solute free. Simulations were carried out for soil hydraulic properties representing a loamy soil (according to a HYDRUS catalog).

Description of the simulated scenarios

Simulations were carried out for 28 days (4 weeks) to show the combined/cumulative effects of multiple irrigation/fertigation cycles. Irrigations were applied every 7 days (once per week; unless indicated otherwise) with the irrigation flux set at 1200 Lh^{-1} $furrow^{-1}$ for a 100 m long furrow, corresponding to an area based application rate of 12 mm h^{-1}, or to a flux of 60 cm^2h^{-1} in our two-dimensional domain. Contrary to Siyal et al. (2012) who used the so-called 'switch-off depth' to end the irrigation event, in this study we applied a pre-set amount of irrigation at a fixed 7 day cycle. We compared the effects of two different amounts of irrigation by setting the duration at either 4 or 6 h. This gives irrigation volumes that correspond to 69 % (4 h × 60 cm^2 h^{-1} × 2 = 480 cm^2/week) and 103 % (6 h × 60 cm^2 h^{-1} × 2 = 720 cm^2/week) of total ET_p, respectively.

The same soil surface treatments as in Siyal et al. (2012) were considered in this study (see Fig. 2 in Siyal et al. (2012)). The soil at the furrow bottom was either (a) untreated, i.e., it remained in standard conditions with normal soil hydraulic properties (S_o), which served as the control, (b) compacted with its hydraulic conductivity of the top 2 cm of soil reduced by 80 % (S_c) compared with the control, or (c) was covered with an impermeable membrane so that the hydraulic conductivity was zero at the bottom of the furrow (S_p).

Since it may be difficult to maintain surface plastic on the base of the furrow while allowing access to the field by agricultural machinery, the S_p treatments were rerun for situations where both the plastic and irrigation are present only in alternate furrows, while the in-between furrow retains its natural condition (S_o). For the alternate furrow irrigation, we considered three scenarios. In scenario one (S_{a1}), the same duration of irrigation was used as for the S_p treatments, which resulted in half of the irrigation water being applied to the field. In scenario two (S_{a2}), the duration of irrigation was doubled, which resulted in the same amount of irrigation water being applied to the field as for the S_p treatments. In scenario three (S_{a3}), the same duration of irrigation was used as for the S_p treatments, but the frequency of irrigation was doubled (i.e., irrigation occurred every 3.5 days), which resulted in the same amount of irrigation water being applied to the field as for the S_p treatments.

Four fertigation strategies were considered. The first three involved 1 h fertigation events, applied at the beginning (*B*), in the middle (*M*) and at the end (*E*) of the irrigation cycle. The fertigation at the end was started 1.5 h before the end of the irrigation cycle to allow half an hour without fertigation before ending the irrigation cycle. The fourth fertigation strategy involved application of fertigation throughout the irrigation cycle. Simulations were carried out using a dimensionless solute concentration, and the solute concentration of the irrigation water was selected so that 100 units of mass were applied during the 1-month simulations (i.e., during the four irrigation cycles). This allows us to present calculated solute fluxes, such as leaching and root uptake, as a percent of the total applied. For the 1-h long fertigations, the solute concentration in irrigation water was calculated as:

$$S_c = n_f n_{ir} Q_p C_p t_p$$

and

$$C_p = \frac{S_c}{n_f n_{ir} Q_p t_p} = \frac{100}{2(\text{half - furrows}) \times 4(\text{irrigation cycles}) \times 60(\text{m}^2/\text{h}) \times 1(\text{h})} = 0.20833 \quad (7)$$

where n_f is the number of half-furrows in the transport domain, n_{ir} is the number of irrigation cycles, and t_p is the duration of fertigation [T]. Concentrations were lowered appropriately for the continuous fertigation. We would like to emphasize that our current model considers only processes in the plane perpendicular to a furrow and neglects processes along the furrow, such as the advancement and/or recession of the irrigation water front.

Results and discussion

Dynamics of the water and solute mass balance in the furrow

First, we will evaluate the functioning of the newly developed "Furrow" module and its coupling with the HYDRUS (2D/3D) model during one irrigation/fertigation cycle. We will describe both water and solute mass balances, as well as all main fluxes into/out of the furrow.

Figures 3, 4, 5, 6 and 7 show the dynamics of water and solute in the furrow during one irrigation cycle for

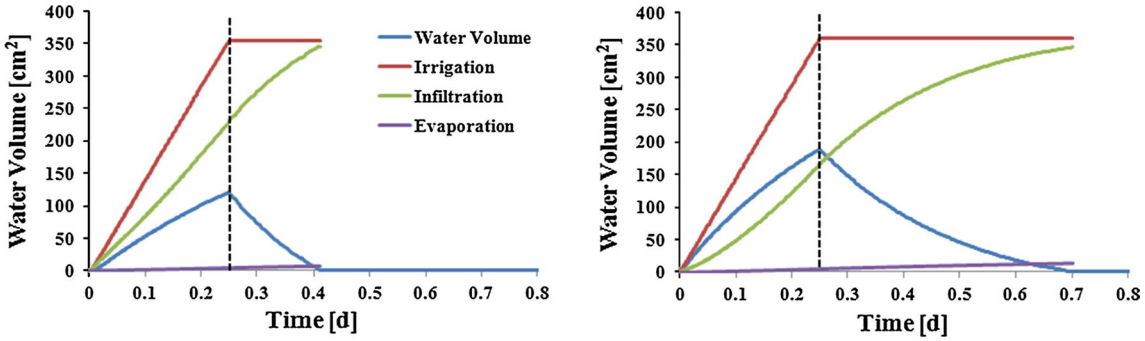

Fig. 3 Volume of water in the (half) furrow, and cumulative irrigation, infiltration, and evaporation fluxes for treatments S_o (*left*) and S_p (*right*). The end of irrigation (0.25 day) is indicated by a *vertical dashed line*. The end of infiltration (when all water infiltrated into the soil profile) is at about 0.41 day (*left*) and 0.70 day (*right*)

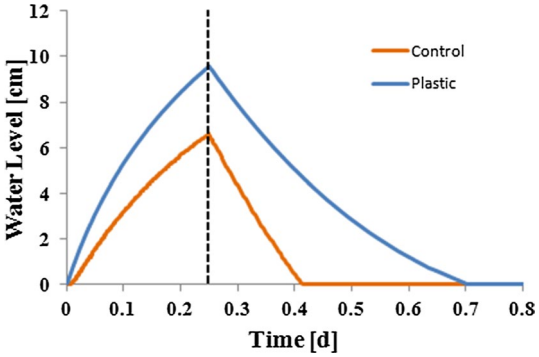

Fig. 4 Water level in the furrow during one irrigation cycle for treatments S_o (normal) and S_p (plastic). The end of irrigation (0.25 day) is indicated by a *vertical dashed line*

treatments with either the standard untreated bottom of the furrow (S_o; referred to as the "control") (left) or with the impermeable membrane placed on the bottom of the furrow (S_p; referred to as "plastic") (right). Irrigation is applied at a rate of 60 cm^2/h for 6 h and fertigation is applied at a dimensionless concentration of 0.20833 during 1 h either at the beginning of irrigation, in the middle of irrigation, or 1.5 h before the end of irrigation. This concentration will provide 100 units of fertigation during four irrigation cycles (0.20833 × 4 irrigation cycles × 2 half-furrows × 60 cm^2/h × 1 h = 100 cm^2 = 100 %). Potential evapotranspiration is equal to 1 cm/day.

Water balance and fluxes

Figure 3 shows cumulative irrigation, infiltration, and evaporation fluxes to/from the (half) furrow, as well as the water volume in the furrow during one irrigation cycle. Figure 4 shows the water level and Fig. 5 shows the irrigation and infiltration fluxes during the same time. Irrigation is applied for 6 h (0.25 day) and water infiltrates from the furrow to the soil profile for about 10 h (0.41 day) in treatments S_o and about 18.5 h (0.70 day) in treatments S_p. Since the irrigation flux is larger than the infiltration flux (Fig. 5), the water volume and the water level in the furrow increases during the first 6 h (Figs. 3, 4). Once irrigation stops, the water level starts to decrease, until all water infiltrates (Figs. 4, 5). The dynamics in the water level (Fig. 4) is closely linked with the volume of water in the furrow (Fig. 3). It increases faster in the furrow with the plastic at

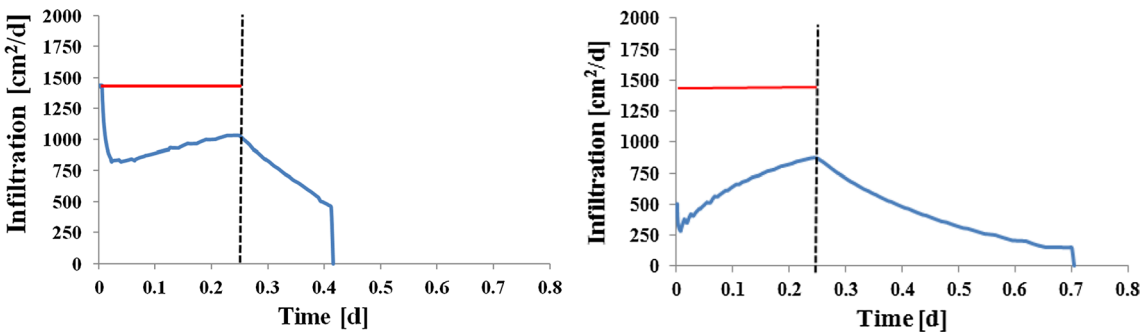

Fig. 5 Irrigation (*red*) and infiltration (*blue*) fluxes [cm^2/day] during one irrigation cycle for treatments S_o (*left*) and S_p (*right*). The end of irrigation (0.25 day) is indicated by a *vertical dashed line*

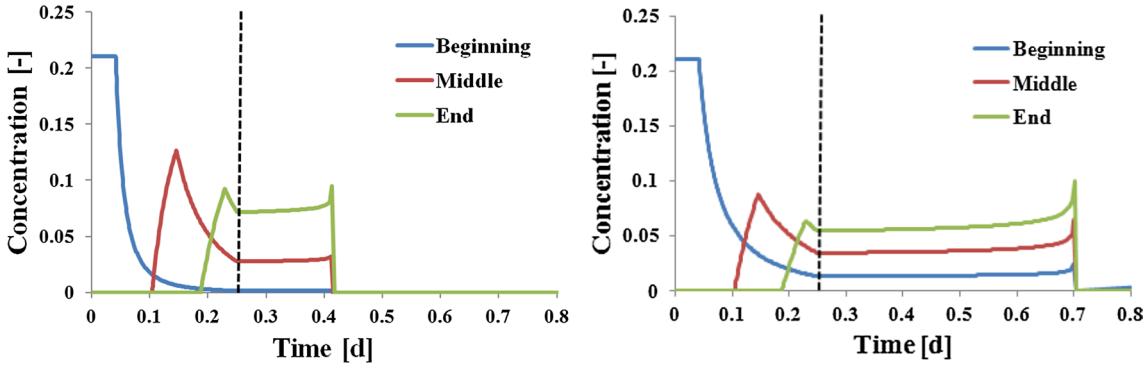

Fig. 6 Concentrations in furrow water during one irrigation cycle when fertigation is applied either at the *Beginning*, in the *Middle*, or at the *End* of irrigation for treatments S_o (*left*) and S_p (*right*). The end of irrigation (0.25 day) is indicated by a *vertical dashed line*

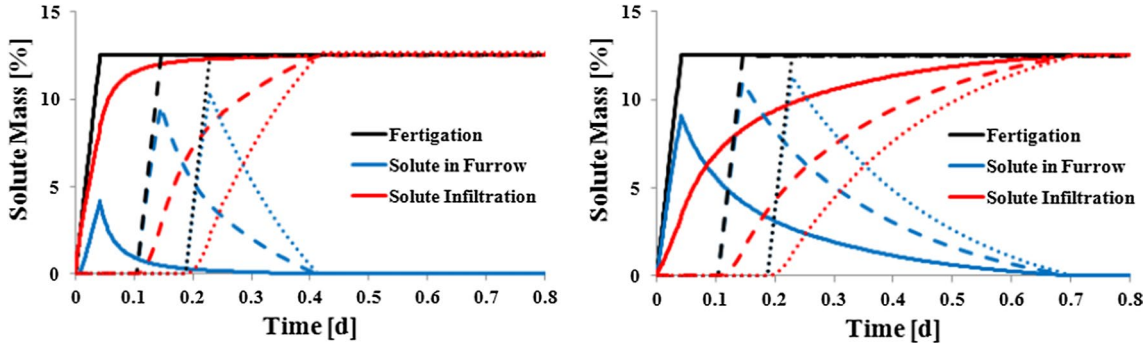

Fig. 7 Solute mass applied (Fertigation; *black line*), solute mass in furrow water (Solute in Furrow; *blue line*), and solute mass infiltrated (Solute Infiltration; *red line*) during one irrigation cycle when fertigation is applied either at the beginning (*solid lines*), in the middle (*dashed lines*), or at the end (*dotted lines*) of irrigation for treatments S_o (*left*) and S_p (*right*)

the bottom (S_p) because of reduced infiltration compared to the S_o treatments (Fig. 4). On the other hand, the subsequent decrease in the water level (volume) is significantly slower in the S_p treatments compared to the S_o treatments, again due to reduced vertically downward infiltration (Fig. 4). Evaporation is considerably smaller than the other fluxes (Fig. 3). The volume of water in the furrow is thus approximately equal to the difference between cumulative irrigation and cumulative infiltration (Fig. 3).

Figure 5 shows that the infiltration process is complex in furrow irrigation. In the S_o treatments, initially all applied irrigation water infiltrates into the soil profile and thus infiltration and irrigation fluxes are the same. Once water starts ponding in the furrow, the infiltration curve follows a typical hyperbolic curve, similar to that for one-dimensional infiltration from ponding (e.g., Kostiakov, Philip and Horton, etc.). However, as the water level in the furrow increases, a larger surface area becomes active in the infiltration process (not only the bottom of the furrow, but also increasingly on the sides of the furrow), and the infiltration rate starts increasing. Once irrigation stops, the water level in the furrow starts decreasing, and so does the infiltration rate, until it becomes zero once all water has infiltrated.

In the S_p treatments, the initial infiltration rate is much smaller than for the S_o treatments because the bottom of the furrow is impermeable and only a small fraction of the furrow sides are exposed to ponding water. As for the S_o treatments, as the water level in the furrow increases a larger surface area becomes active in the infiltration process, and the infiltration rate starts increasing. Once irrigation stops, the water level in the furrow starts decreasing, and so does the infiltration rate, albeit at a much slower rate than for the S_o treatments due to the impermeable bottom, until it becomes zero when all water has infiltrated.

Solute balance and concentrations

Fertigation is applied at a dimensionless concentration of 0.20833 during 1 h either at the beginning of irrigation, in the middle of irrigation, or 1.5 h before the end of irrigation. During one irrigation cycle, the applied solute mass to one half-furrow is 12.5 % (0.20833 × 60 cm^2/h × 1 h = 1

2.5 cm^2). Figures 6 and 7 show results for all three fertigation strategies. It is assumed that there is a complete mixing of water in the furrow (applied irrigation water is instantaneously mixed with water already in the furrow) so the concentration can be represented by a single value.

Figure 6 shows the average solute concentrations in the furrow for the three fertigation strategies. When solute is applied at the beginning of the irrigation cycle (Fig. 6; Beginning), the concentration in the furrow water is equal to the concentration in the irrigation water. Once fertigation stops and infiltration continues, water in the furrow is quickly diluted by continued inflow of irrigation water and the concentration decreases rapidly. When solute is applied later in the irrigation cycle (Fig. 6; Middle and/or End), incoming irrigation water mixes with the volume of water already in the furrow so the highest concentrations that are reached have lower values than when fertigation is applied at the beginning of the irrigation cycle. Once infiltration stops (at 0.25 day), furrow concentrations stop decreasing and remain more or less the same. There is only a small increase in concentration during this period (after irrigation stops and the remaining furrow water keeps infiltrating into the soil profile) as a result of evaporation, which concentrates solutes in the furrow water. This effect, which is relatively minor, is much more pronounced for the S_p treatments because of the slower infiltration rates and longer duration of the infiltration process.

Figure 7 shows the solute mass in the furrow and cumulative fertigation and infiltration fluxes. When solute is applied at the beginning of the irrigation cycle, it immediately infiltrates into the soil profile, so less solute mass is stored in the furrow. When solute is applied later in the irrigation cycle and mixes with water in the furrow, the initial furrow concentrations are lower than when solute is applied at the beginning (Fig. 6). Consequently, solute infiltrates slower into the soil profile and more solute is stored in the furrow over longer periods of time (Fig. 7). At the end of the irrigation cycle, all water infiltrates into the soil profile and thus the final solute mass is equal to zero and solute mass applied (fertigation) and infiltrated are the same.

Dynamics of the water and solute mass balance in the soil

Water fluxes

Table 1 shows the cumulative values of the different hydrological fluxes and the change in water storage in the transport domain, the duration of irrigation and infiltration, water-use efficiency (WUE), and the plant yield for the 6- and 4-h irrigations for the S_o, S_c, S_p treatments and S_a scenarios (during the first irrigation cycle). Note that in Table 1, the plant yield is defined as the ratio of the actual to potential transpiration, expressed as a percentage ($=100 \times T_a/T_p$), and that drainage is reported at a depth of −100 cm, i.e., at the bottom of the soil profile.

Values in Table 1 can be compared with the total amount of applied irrigation water (60 cm^2/h × 0.25(0.1666) da y × 24 h × 2 half-furrows × 4 irrigation cycles = 2880 (1920) cm^2 for 6 (4) hour irrigations), cumulative potential transpiration (0.8 cm/day × 40 cm × 28 day = 896 c m^2), cumulative potential evaporation from the surface of the ridge (0.2 cm/day × 40 cm × 28 day = 224 cm^2) and cumulative potential evaporation from the furrow (1.0 cm/day × 60 cm × 28 day = 1680 cm^2).

Table 1 shows that although irrigation volume is the same in all three standard treatments (S_o, S_c, and S_p) and two alternate furrow scenarios (S_{a1} and S_{a3}), infiltration is different, because water is lost from the furrow due to evaporation (ET_p) from the water surface. Since water stays the longest in the furrow with the plastic bottom (see Infiltration duration), most water is lost via evaporation in this scenario, and least water infiltrates into the soil profile (about 3 % less), compared to the control. Similar effects can also be seen for the alternate furrow S_a scenarios, with longer residence time of water in the furrow, but with a smaller surface exposed to evaporation.

Infiltration durations increase with increased restrictions on direct downward infiltration from the base of the furrow in the S_o treatment to the S_c and S_p treatments. Infiltration durations are practically the same for the S_p treatment and the S_{a1} and S_{a3} treatments, which all have the plastic bottom and the same irrigation volume. This is because reported irrigation durations are for the first irrigation cycle, when infiltration fronts from the two neighboring furrows of the S_o treatment do not overlap and are thus similar to those from alternative furrows (the S_{a1} and S_{a3} treatments).

Since root water uptake is optimal only for pressure heads between the two stress response function pressure heads h_2 (= −25 cm) and h_3 (= −200 cm) and is reduced for pressure heads outside of this interval, actual root water uptake is always reduced from its optimal value (T_p = 0.8 cm/day) (Fig. 8). Root water uptake is reduced not only immediately after irrigation, since the pressure head around the furrow is higher than h_2, but also after irrigation stops because then a part of the root zone becomes drier than h_3. Figure 8 shows that plants are less stressed in the S_p treatment (right) than in the S_o treatment (left), reflecting better root zone distribution of water and its availability in this treatment (Fig. 9). Figure 9 shows that while in the S_o treatment water infiltrates predominantly downward and thus out of reach of plant roots, in the S_p treatment, in which vertically downward infiltration is prevented, water moves predominantly sideways into the root zone and upward into the ridge, increasing root water uptake. Note that there is very little stress in the

Table 1 Cumulative fluxes (cm^2) over 28 days (4 irrigation cycles) for 6 (top) and 4 (bottom) hour irrigations for the S_o (control), S_c (compacted), S_p (plastic) treatments and the S_a (alternate furrow) scenarios

Fluxes	Furrow treatments			Alternate furrow scenarios		
	Control, S_o	Compacted, S_c	Plastic, S_p	S_{a1}	S_{a2}	S_{a3}
6-h irrigations						
Infiltration	2880	2824	2775	1387	2787	2770
Transpiration	−828	−836	−870	−664	−802	−770
Evaporation from ridge	−27	−67	−99	−41	−90	−104
Evaporation from furrow	−637	−605	−422	−213	−239	−335
Drainage	−687	−582	−579	−152	−1027	−788
Change in storage	700	731	806	320	633	772
Yield (%)	92.4	92.7	97	74.1	89.5	85.9
WUE (%)	28.3	29	31.1	46.1	27.8	26.7
Irrigation duration (day)	0.25	0.25	0.25	0.25	0.5	0.25
Infiltration duration (day)	0.4128	0.5428	0.699	0.699	1.068	0.699
4-h irrigations						
Infiltration	1920	1889	1864	943	1853	1841
Transpiration	−727	−733	−819	−567	−731	−684
Evaporation from ridge	−6	−25	−34	−19	−59	−57
Evaporation from furrow	−551	−527	−357	−189	−227	−312
Drainage	−128	−78	−59	−27	−385	−253
Change in storage	529	530	576	122	455	535
Yield (%)	81.1	81.8	91.4	63.3	81.5	76.3
WUE (%)	37.9	38.2	42.7	59.1	38.1	35.6
Irrigation duration (day)	0.16666	0.16666	0.16666	0.16666	0.3333	0.16666
Infiltration duration (day)	0.2885	0.4082	0.537	0.537	0.833	0.537

Scenarios S_{a2} have 12- and 8-h irrigations. Additional information includes the duration (day) of irrigation and infiltration, change in water storage in the transport domain (cm^2), the plant yield (%), and the water-use efficiency (WUE) (%)

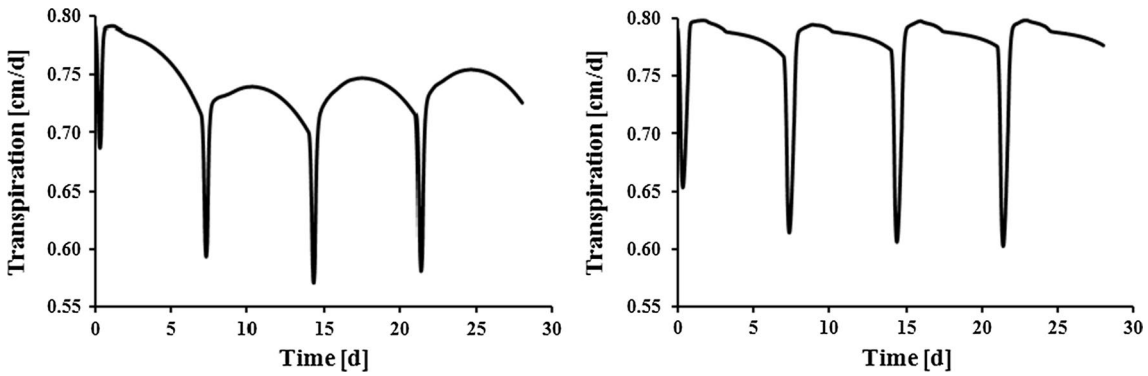

Fig. 8 Actual transpiration rate (= root water uptake) for the 6-h irrigation for treatments S_o (*left*) and S_p (*right*)

S_p treatment ($T_a \approx T_p$, Fig. 8), in which water contents in the entire soil profile, except for the shallow surface layer of the ridge, are above field capacity. This is also obvious from the cumulative transpiration values shown in Table 1, which display an increase in transpiration with the reduction in the downward flow through the bottom of the furrow (from treatments S_o, to S_c, and S_p). There is a further reduction in transpiration for the S_a scenario (alternate furrows with plastic and irrigation), since part of the root zone, furthermost from the furrow with plastic and irrigation, is not fully supplied with water, resulting in water contents below field capacity and reduced root water uptake (see Fig. 9). While there is a reduction in transpiration in the alternate furrow S_a scenarios, in which the same amount of water is applied as in the original scenarios (i.e., in S_{a2} and S_{a3}), this

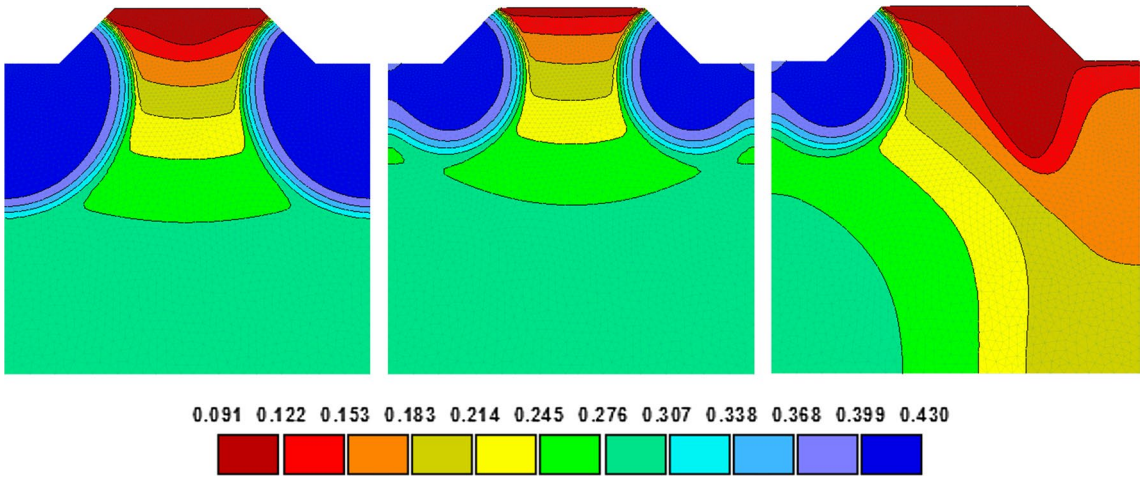

Fig. 9 Soil water content profiles ($t = 6$ h in the last irrigation cycle) for the control treatment S_o (*left*), the treatment with plastic S_p (*middle*), and the scenario with alternate furrow irrigations S_a (*right*)

reduction is only in the order of 10 % compared to the S_p treatment and 3–7 % compared to the S_o treatment.

The same trend is also displayed by the corresponding yield values. Yield is considerably higher for the S_p treatment compared to the S_o treatment, by 4 and 10 % for the 6- and 4-h irrigations, respectively. Yield for the 4-h irrigation of the S_p treatment is almost the same as yields for the 6-h irrigation for the S_o and S_c treatments. Yield for the S_{a2} scenarios (alternate furrows; double irrigation duration) is similar to the S_o treatment, since the positive effect of plastic in all furrows is reduced when it is present only in alternate furrows and irrigation durations have to be extended to provide the same amount of water. As with transpiration, yields for the alternate furrow scenarios, in which the same amount of water is applied as in the original treatments (i.e., in the S_{a2} and S_{a3} scenarios), are reduced by roughly 10 % compared to the S_p treatment and of 3–7 % compared to the S_o treatment (Table 1). It should be noted that when only half the water is applied in the S_{a1} scenarios compared to the original treatments, the reduction in yield is less than 20 % compared to the S_o treatment, producing considerably higher water-use efficiency, which may be important in situations where water resources are limited. It should also be noted that our simulations probably underestimate yield for the alternate furrow scenarios, since plant roots are likely to adjust to receiving irrigation from only alternate furrows, which is a process that our simulations do not include.

Water-use efficiency (WUE) is typically defined as the ratio of crop biomass produced to the total water transpired by the plant (Bacon 2004). Since we do not have a plant growth model that calculates biomass produced, we cannot report water-use efficiency using this definition. Rather, we report WUE in Table 1 as the percentage of water transpired by the plants relative to the total irrigation water. Note that this definition underestimates WUE since it considers a change of storage over considered time period as water lost. Similarly, to the discussion above on yield, WUE increases with a reduction in the amount of irrigation water that infiltrates directly below the furrow and is considerably higher for the S_p treatment compared to the S_o treatment, for both 6 and 4-h irrigations. WUE is higher by about 9–10.5 % for 4-h irrigations compared to 6-h irrigations, although this increase is at the expense of yield. Less water (percentagewise) is lost to evaporation and drainage and more is used for transpiration for 4-h irrigations compared to 6-h irrigation. The highest WUE, i.e., the largest fraction of irrigation water is used for transpiration, was achieved in the S_{a1} scenario when alternate furrows are used for irrigation and when only half of the total water is applied compared with that applied in scenarios where every furrow is irrigated. WUE for the S_{a2} scenarios (alternate furrows; double irrigation duration) is similar to the S_o treatment. This is because the positive effect of plastic is reduced when it is present only in alternate furrows and irrigation durations have been increased to provide the same amount of water. WUE for the alternate furrow scenarios, in which the same amount of water is applied as in the original treatments (i.e., in the S_{a2} and S_{a3} scenarios), is reduced by about 20 and 5 % compared to the S_{a1} scenario and S_p treatment, respectively (Table 1).

Figure 10 shows evaporation from the surface of the ridge for the 6-h irrigation for treatments S_o and S_p, while Table 1 gives cumulative evaporation values for all treatments. Since more water flows from the furrow horizontally into the ridge, it is wetter in the S_p treatments compared to the S_o treatments. As a result, considerably more water is lost to evaporation from the surface of the ridge. Evaporation from the ridge surface increases from S_o to S_c

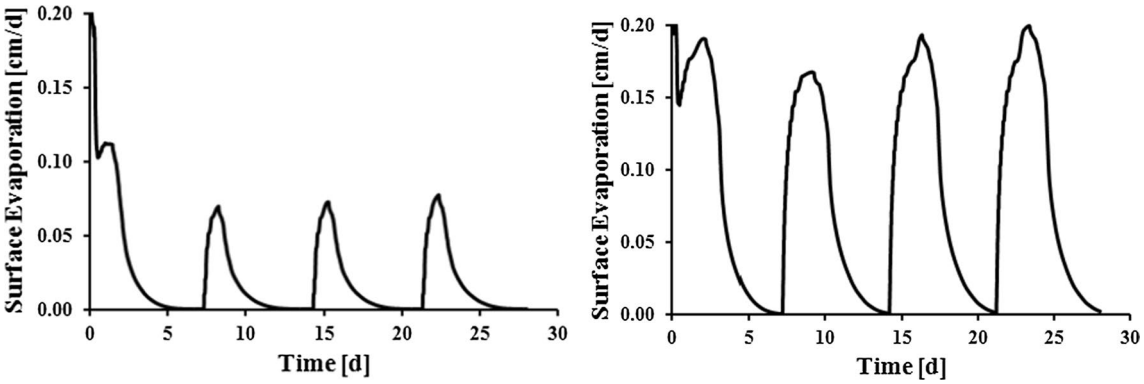

Fig. 10 Actual evaporation flux (cm/day) from the surface of the ridge for the 6-h irrigation for treatments S_o (*left*) and S_p (*right*)

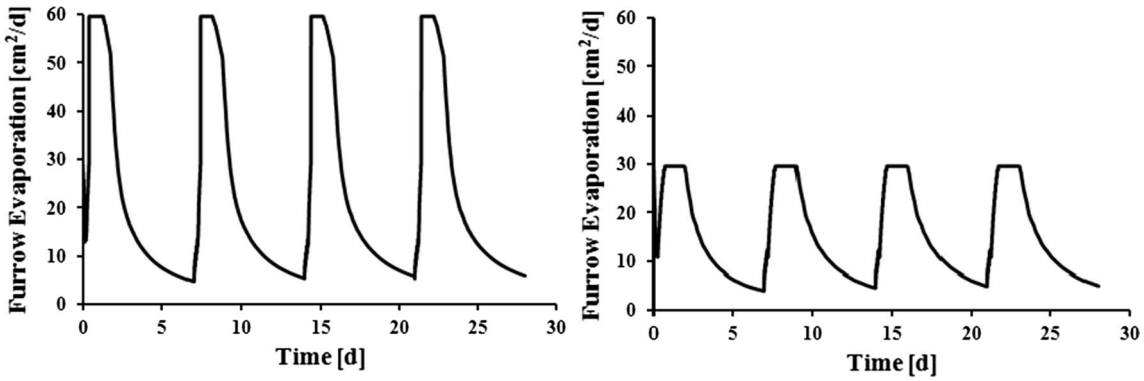

Fig. 11 Actual evaporation flux from the bottom and sides of the furrow for the 6-h irrigation for treatments S_o (*left*) and S_p (*right*)

to S_p (Table 1). It would be beneficial to minimize evaporation from the ridge in the S_p treatment by also covering the ridge surface with a plastic membrane.

Figure 10 also shows the dynamics of the actual evaporation fluxes during the four irrigation cycles. Between irrigations, the soil surface becomes dry and evaporation is reduced to almost zero. After irrigation, the soil surface becomes moist and evaporation increases (compare to $E_p = 0.2$ cm/day). The first irrigation cycle shows higher evaporation due to the relatively high initial soil water content than during the following three irrigation cycles, during which the evaporation patterns are similar. Note that during the first irrigation cycle, contrary to the other irrigation cycles, the actual evaporation is initially equal to the potential evaporation, since the initial pressure head at the soil surface was assumed to be −300 cm, which does not limit evaporation, while at the beginning of the other irrigation cycles the soil surface was very dry, and thus limiting evaporation. Also note that there is a slight increase in evaporation rates between the second and forth irrigation cycles. This is a result of the gradual increase in water storage after each irrigation, which contributes to the increasing soil evaporation with time.

Figure 11 shows the evaporative flux from the bottom and sides of the furrow. The horizontal projection of this boundary (exposed to evaporation) is 60 cm and thus the potential flux is 60 cm^2/day. In the S_p treatments, the bottom of the furrow is covered with plastic so only 30 cm of the boundary is exposed to evaporation. During irrigation, part of the furrow is filled with water and evaporation is limited only to the sides above the water level. Once the furrow is empty, evaporation takes place from the entire furrow (bottom and sides; 60 cm) in the S_o treatments and only through the sides (30 cm) of the furrow in the S_p treatments. Once irrigation stops, evaporation is high, since the bottom and sides of the furrow are wet. Evaporation gradually decreases between irrigations as the bottom and sides of the furrow become dry after the critical evaporation pressure head is reached (Fig. 11). Cumulative soil evaporation from the furrow is highest for the S_o treatments and smallest for the S_p treatments (Table 1). Cumulative evaporation from the furrows is considerably lower for the S_a scenarios (Table 1), since evaporation from the dry furrow is insignificant and evaporation occurs predominantly from the side of the irrigated furrow with the plastic bottom.

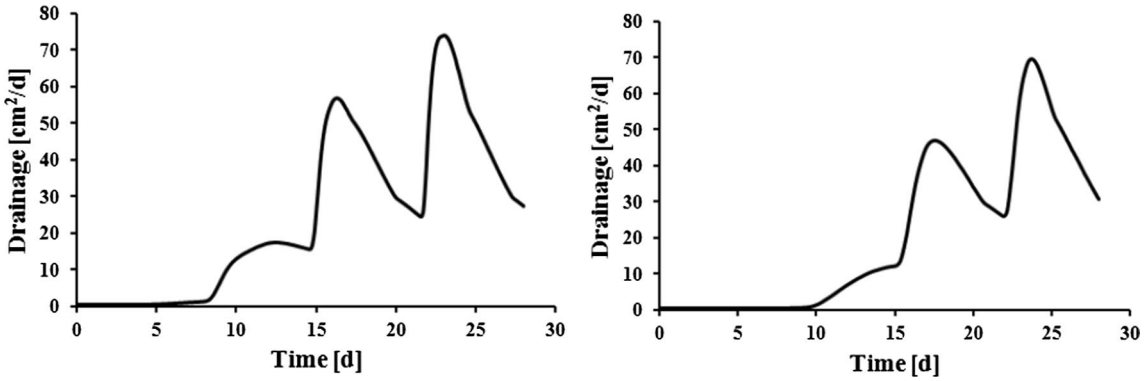

Fig. 12 Deep drainage flux at the bottom of the soil profile for the 6-h irrigation for treatments S_o (*left*) and S_p (*right*)

Figure 12 and Table 1 shows that drainage is considerably higher for the S_o treatments than for the other two treatments (S_c and S_p). In the S_o treatments, most water infiltrates vertically downward through the bottom of the furrow and moves unhindered toward the bottom of the profile, bypassing the bulk of the crop root zone. In the two other treatments, vertically downward infiltration is either reduced (S_c) or completely eliminated (S_p). Consequently, greater fractions of applied water move horizontally into the broader root zone and upward into the ridge. On the other hand, drainage is considerably higher in the S_a scenarios, in which the same amount of irrigation water is applied [either by doubling the irrigation time (S_{a2}) or irrigation frequency (S_{a3})] as in the original treatments. This is because the application of water is less well distributed by being applied only to alternate furrows. Obviously, there is much less drainage in the S_{a1} scenario (Table 1), in which only half the amount of irrigation water was applied. Figure 12 also shows that drainage is relatively small during the first irrigation cycle and then increases with each irrigation cycle as more of the applied irrigation water reaches the bottom of the soil profile. This figure also shows that the analysis of only one irrigation cycle (which is the case for many of the studies discussed in the Introduction) cannot provide a full picture of the processes and cumulative effects occurring in the root zone and soil profile.

Solute fluxes

Table 2 shows various components of the solute mass balance, such as cumulative root solute uptake, cumulative solute leaching (at a depth of 100 cm), and the change in solute mass in the transport domain for the 4- and 6-h irrigations for the three surface treatments (S_o, S_c, and S_p), as well as for the alternate furrow irrigation scenarios (S_{a1}, S_{a2}, and S_{a3}), and the four fertigation strategies.

Table 2 shows that for the S_o treatment and 6-h irrigation, solute leaching is highest (8.8 %) and lowest (5.6 %) when fertigation is applied at the beginning and the end of the irrigation cycle, respectively. Similar leaching is obtained when fertigation is applied either in the middle (6.3 %) or continuously (6.7 %) throughout the entire irrigation cycle. These observations are similar to those of Gärdenäs et al. (2005), who also concluded for different micro-irrigation schemes that fertigation applied at the beginning of an irrigation cycle tends to increase nitrate leaching and that fertigation applied at the end of an irrigation cycle tends to reduce nitrate leaching. Note that similarly to Gärdenäs et al. (2005), and contrary to Cote et al. (2003) who studied only one irrigation cycle, we have analyzed multiple irrigation cycles. Similarly, Bouwer et al. (1990) and Soroush et al. (2012) concluded that leaching of fertilizers to groundwater can be minimized when fertigation is applied toward the end of an irrigation event.

The highest (23 %) and lowest (18 %) root solute uptake is obtained when fertigation is applied in the middle and at the beginning of the irrigation cycle. Similarly high solute uptakes as when the fertigation is applied in the middle of the irrigation cycle are obtained when the fertilizer is applied continuously. This conclusion is consistent with Playán and Faci (1997), who concluded that applying fertilizer at a constant rate during the entire irrigation event is usually the best solution. Similar relative results are obtained for the S_p treatments, except that root solute uptake is about 4–6 % higher (Fig. 13), and solute leaching is about 2–4 % lower (Fig. 14). There are much smaller differences between different fertigation timings in the S_{a2} and S_{a3} scenarios (with alternate furrows). Root solute uptake is between 20–22 and 26–28 % of the applied volume for the 6- and 4-h irrigations. However, there is much higher leaching for these two alternate furrow scenarios. Solute leaching is considerably higher for the S_{a2} scenarios with 6-h irrigations, ranging between 17 and 23 % when fertigation is applied at the end and at the beginning of the irrigation cycle, respectively. There is higher root solute uptake (by about 8 and 4 % for 6- and

Table 2 Components of the solute mass balance including fertigation (%), root uptake (%), leaching (%), and change in storage (%) over 28 days (4 irrigation cycles) for 6- and 4-h irrigations for the S_o (control), S_c (density), S_p (plastic) treatments, and the S_a (alternate furrow plastic) scenarios, with fertigation applied at the beginning (B), in the middle (M), at the end (E), or continuously (F) throughout the irrigation cycle

	Treatments											
	Control, S_o				Compacted, S_c				Plastic, S_p			
Fertigation timing	B	M	E	F	B	M	E	F	B	M	E	F
6-h irrigations												
Fertigation (%)	100	100	100	100	100	100	100	100	100	100	100	100
Root uptake (%)	18	23	21	22	21	24	23	23	26	27	26	27
Leaching (%)	8.8	6.3	5.6	6.7	6.0	4.4	4.0	4.6	4.4	3.8	3.5	3.8
Change in storage (%)	69	71	75	72	71	72	75	73	69	70	72	71
4-h irrigations												
Fertigation (%)	100	100	100	100	100	100	100	100	100	100	100	100
Root uptake (%)	21	25	24	24	24	27	26	26	30	32	31	31
Leaching (%)	0.5	0.3	0.3	0.4	0.1	0.1	0.1	0.1	0.0	0.0	0.0	0.0
Change in storage (%)	78	75	76	76	75	75	76	75	66	69	70	69
	Alternate furrow scenarios											
	S_{a1}				S_{a2}				S_{a3}			
Fertigation timing	B	M	E	F	B	M	E	F	B	M	E	F
6-h irrigations												
Fertigation (%)	100	100	100	100	100	100	100	100	100	100	100	100
Root uptake (%)	29	30	30	30	20	23	21	22	21	22	21	22
Leaching (%)	1.7	1.4	1.2	1.4	23	19	17	19	15	13	13	14
Change in storage (%)	69	69	71	70	56	59	63	59	64	65	67	65
4-h irrigations												
Fertigation (%)	100	100	100	100	100	100	100	100	100	100	100	100
Root uptake (%)	28	31	29	29	26	28	26	27	26	26	26	26
Leaching (%)	0.0	0.0	0.0	0.0	7.3	5.9	5.3	6.0	3.2	2.9	2.8	3.0
Change in storage (%)	72	71	71	70	66	67	70	68	71	72	73	72

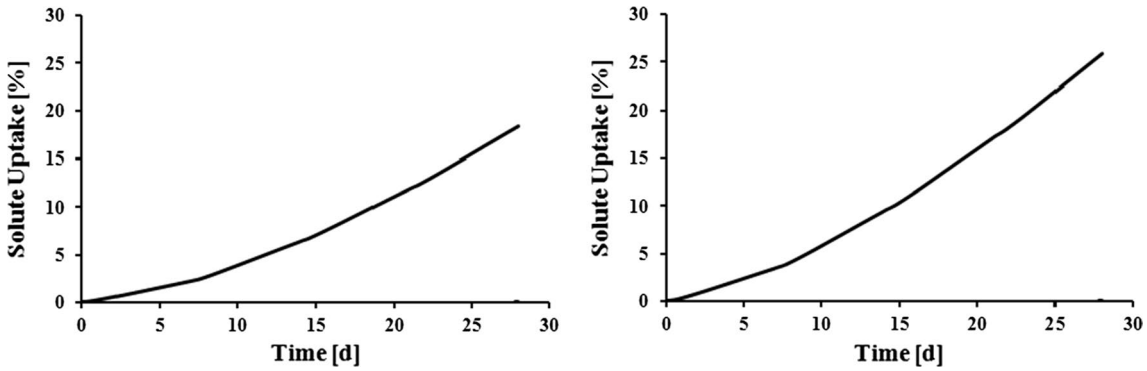

Fig. 13 Cumulative root solute uptake for the 6-h irrigation for treatments S_o (*left*) and S_p (*right*) when fertigation is applied at the beginning of the irrigation cycle

4-h irrigations, respectively) for the S_{a1} scenarios, compared to all other scenarios. Since only half of the irrigation water is applied in these scenarios, there is only limited leaching below the root zone and fertilizers remain accessible to the plant roots. Note that the numbers in columns of Table 2 do not always add up to 100 %, due to rounding errors and small mass balance errors (up to 2 %) in numerical calculations.

Figure 15 shows the concentration profiles at the end of the simulations for the S_o and S_p treatments and S_{a2} scenarios. While in the S_p treatment, the concentrations are the highest along the surface of the ridge due to the effects of

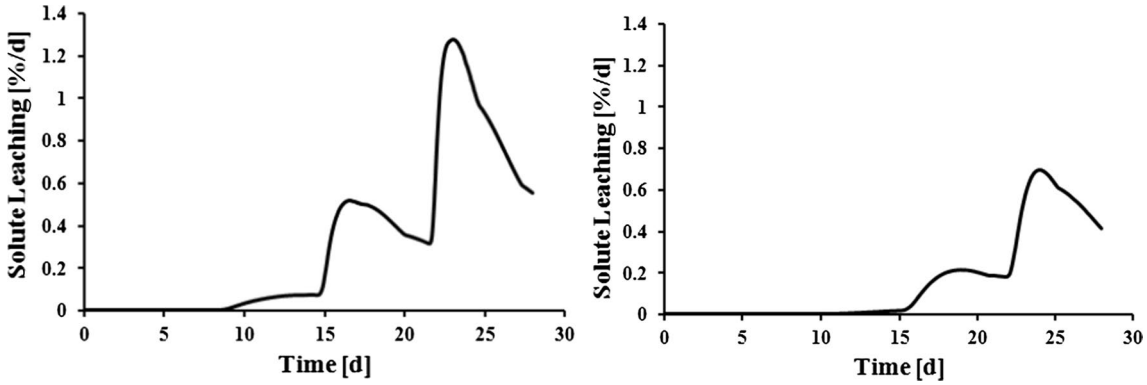

Fig. 14 Cumulative solute leaching for the 6-h irrigation treatments S_o (*left*) and S_p (*right*) when fertigation is applied at the beginning of the irrigation cycle

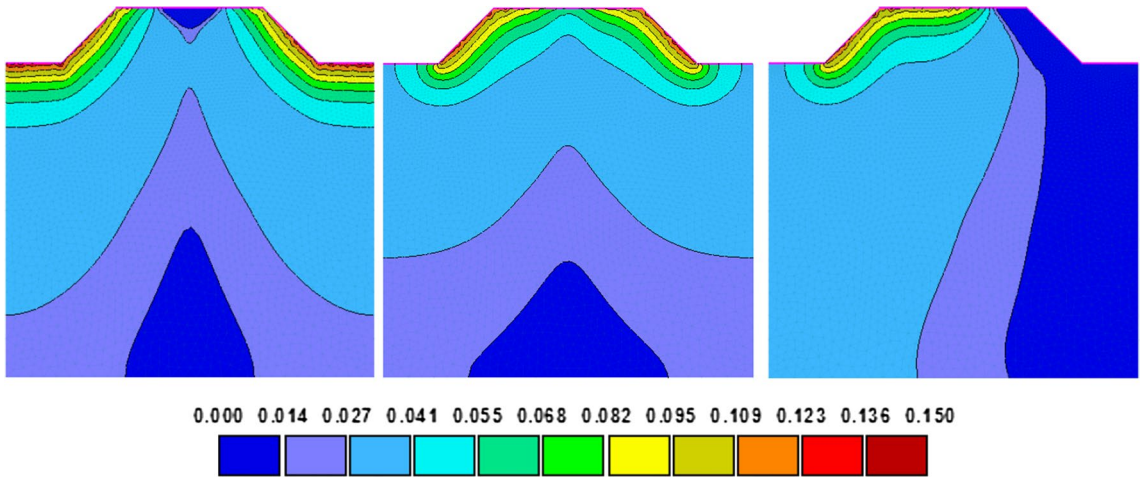

Fig. 15 Concentration profiles ($t = 28$ days) for treatments S_o (*left*) and S_p (*middle*), and scenario S_{a2} (*right*)

evaporation and relatively low at the bottom of the furrow where evaporation is prevented by the plastic cover, in the S_o treatment, the concentrations are the highest along the surface of the furrow (both bottom and sides) since evaporation occurs on all these surfaces. However, some solute, below the bottom of the furrow, is outside of the rootzone and thus out of reach of plant roots in the S_o treatment. In the S_o treatment, the concentrations are the lowest in the middle of the ridge, since very little infiltration water reaches this part of the soil profile, which is relatively dry throughout the simulation. Both these factors reduce root solute uptake for the S_o treatment. Figure 15 also shows that fertilizer does not reach the entire root zone when irrigation is applied in only one furrow (in the S_{a2} scenario), resulting also in lower root solute uptake (Table 2). Significantly more pronounced vertical movement of fertilizer in the S_o treatment compared to the S_p treatment is also apparent in Fig. 15. Even more pronounced vertical movement is apparent for the S_{a2} scenario, in which double the amount of water and solute is applied in one (left) plastic covered furrow.

Table 2 also shows that the results are qualitatively similar for the 4-h irrigation scenarios, except that root solute uptake is about 2–4 % higher and solute leaching is virtually eliminated (below 1 % for all treatments except for the alternate furrow scenarios).

Figure 14 shows that solute leaching starts earlier for the S_o treatment (after about 8 days) than for the S_p treatment (after about 15 days) and also that solute leaching fluxes are higher for the S_o treatment than for the S_p treatment (see also Table 2). Figure 14 also shows that the dynamics of solute fluxes is similar to water fluxes (Fig. 12). Solute leaching fluxes clearly reflect the irrigation cycles.

Figure 16 shows that root solute uptake gradually increases as solute spreads through the root zone, which was initially solute free, and thus becomes more available to plant roots. This function is simply a derivative of the function displayed in Fig. 13. Note the short dips in root

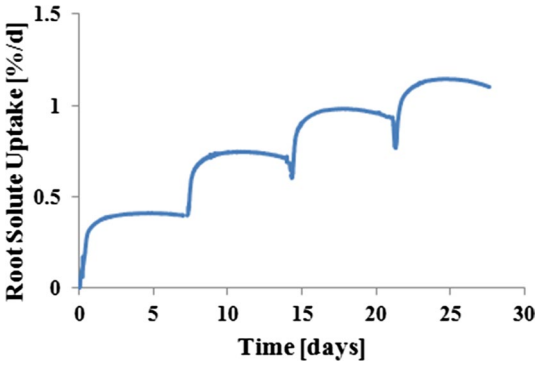

Fig. 16 Root solute uptake for the 6-h irrigation treatment S_o when fertigation is applied at the beginning of the irrigation cycle

solute uptake immediately after the beginning of irrigations. These are caused by a reduction in root water uptake due to water stress that results from oversaturation of a part of the root zone. Figure 16 suggests that cumulative fertilizer uptake given in Table 2 would be higher if the root zone had been supplied with fertilizer from the very beginning, rather than assuming it was solute free.

Conclusions

We have developed a furrow irrigation submodule for HYDRUS (2D/3D), which considers processes including irrigation, infiltration, evaporation and fertigation. Using these fluxes and the mass balance calculations, this submodule calculates the water level and solute concentration in the furrow and dynamically adjusts boundary conditions for the soil transport domain. The resulting coupled model was used to assess the effects different soil surface management strategies and different timings of fertigation had on root water and solute uptake along with deep drainage and solute leaching over a 1-month time period.

Our simulations showed that more water was available for transpiration for treatment S_p with zero infiltration through the bottom of the furrow compared with the normal furrow bottom control treatment (S_o). As a result, a higher yield (with an increase from 92 to 97 % of potential transpiration) was also obtained for the S_p treatments. In contrast, a larger fraction of applied water was lost due to evaporation from water taking longer to infiltrate from the furrow but less water drained from the root zone for the S_p treatments compared with the control (S_o) or compacted furrow bottom (S_c).

Simulations for the S_{a2} and S_{a3} scenarios with plastic and irrigation in alternate furrows and the same amount of applied water as in the standard S_p treatments showed a reduction in transpiration and yield, more water lost due to deep drainage, but much less water lost due to evaporation from the furrow. This could be of interest in some areas if the concern is less about leaching and groundwater pollution and more about reducing evaporative losses and preserving accessible water resources. Similar crop yields were obtained for the alternate furrow scenarios (S_{a2} and S_{a3}) as for the control (S_o) and compacted (S_c) furrow treatments. However, the yield for the S_a scenarios were much lower than for the standard S_p treatments. When only half the water is used for irrigation in the S_{a1} scenarios compared to the original treatments (S_o, S_c, and S_p), the reduction in yield is still less than 20 % compared to the S_o scenario. These scenarios produced considerably higher water-use efficiency, which may be advantage in regions where water resources are limited.

The highest root solute uptake (27 and 32 % for the 6- and 4-h irrigation cycles, respectively) was achieved for the S_p (plastic) treatments when fertigation was applied in the middle of the irrigation cycle. In general, higher root solute uptake was achieved with plastic (S_p), followed by the compacted furrow bottom (S_c) and the normal control furrow bottom (S_o). In general, most solute was taken up by plant roots when fertigation was applied in the middle of the irrigation cycle, followed by fertigation at the end of, or continuously throughout the irrigation cycle. The least amount of solute was taken up when fertigation was applied at the beginning of the irrigation cycle, but the differences were not particularly large (<4 %).

The least amount of solute was leached from the soil profile for the treatment with the plastic bottom (S_p) when fertigation was applied at the end of the irrigation cycle. Considerably more leaching was simulated in the alternate furrow scenarios when the same amount of water was applied as in the original treatments. Higher solute uptake was achieved in the alternate furrow strategy (S_a) than for the normal (S_o) and compacted (S_c) furrow bottom treatments, but it was much lower than for the standard plastic treatment (S_p). The significant benefits that can accrue by using plastic sheeting to eliminate the vertical downward infiltration from the base of the furrow warrants further study, with the aim to deliver practical strategies to further improve water and nutrient management and use in furrow irrigated systems.

The new "furrow" module coupled with HYDRUS (2D/3D) proved to be a powerful tool for analyzing water flow and solute transport processes in the furrow and the soil profile. However, this combined tool still considers processes only in a two-dimensional soil profile perpendicular to the actual furrow. It cannot thus fully account for flow in the third dimension, such as the advance and recession of water in the furrow, and the actual mixing of fertilizer with water in the furrow. Development of a full three-dimensional model that accounts for surface fluxes in the furrow

and all subsurface soil processes discussed above will be required to fully describe complex three-dimensional furrow irrigated systems. Such three-dimensional models could be used to evaluate additional factors such as different slopes.

References

Abbasi F, Šimůnek J, Feyen J, van Genuchten MT, Shouse PJ (2003a) Simultaneous inverse estimation of soil hydraulic and solute transport parameters from transient field experiments: homogeneous soil. Trans ASAE 46(4):1085–1095

Abbasi F, Jacques D, Šimůnek J, Feyen J, van Genuchten MT (2003b) Inverse estimation of the soil hydraulic and solute transport parameters from transient field experiments: heterogeneous soil. Trans ASAE 46(4):1097–1111

Abbasi F, Šimůnek J, van Genuchten MT, Feyen J, Adamsen FJ, Hunsaker DJ, Strelkoff TS, Shouse PJ (2003c) Overland water flow and solute transport: model development and field-data analysis. J Irrig Drain Eng 129(2):71–81

Abbasi F, Feyen J, Van Genuchten MT (2004) Two-dimensional simulation of water flow and solute transport below furrows: model calibration and validation. J Hydrol 290(1–2):63–79

Adamsen FJ, Hunsaker DJ, Perea H (2005) Border strip fertigation: effect of injection strategies on the distribution of Bromide. Trans ASAE 48(2):529–540

Bacon M (2004) Water use efficiency in plant biology. Blackwell Publishing Ltd., Oxford. ISBN 1-4051-1434-7

Benjamin JG, Havis HR, Ahuja LR, Alonso CV (1994) Leaching and water flow patterns in every-furrow and alternate-furrow irrigation. Soil Sci Soc Am J 58(5):1511–1517

Beven KJ, Henderson DE, Reeves AD (1993) Dispersion parameters for undisturbed partially saturated soil. J Hydrol 143:19–43

Bouwer H, Dedrick AR, Jaynes DB (1990) Irrigation management for groundwater quality protection. Irrig Drain Syst 4(4):375–383

Burguete J, Zapata N, García-Navarro P, Maïkaka M, Playán E, Murillo J (2009) Fertigation in furrows and level furrow systems. II: Field experiments, model calibration, and practical applications. J Irrig Drain Eng 135(4):413–420

Cote CM, Bristow KL, Charlesworth PB, Cook FJ, Thorburn PJ (2003) Analysis of soil wetting and solute transport in subsurface trickle irrigation. Irrig Sci 22:143–156. doi:10.1007/s00271-003-0080-8

Crevoisier D, Popova Z, Mailhol JC, Ruelle P (2008) Assessment and simulation of water and nitrogen transfer under furrow irrigation. Agric Water Manag 95(4):354–366

Ebrahimian H, Liaghat A, Parsinejad M, Abbasi F, Navabian M (2012) Comparison of one- and two dimensional models to simulate alternate and conventional furrow fertigation. J Irrig Drain Eng 138(10):929–938. doi:10.1061/(ASCE)IR.1943-4774.0000482

Ebrahimian H, Liaghat A, Parsinejad M, Playan E, Abbasi F, Navabian M (2013a) Simulation of 1D surface and 2D subsurface water flow and nitrate transport in alternate and conventional furrow fertigation. Irrig Sci 31:301–316. doi:10.1007/s00271-011-0303-3

Ebrahimian H, Liaghat A, Parsinejad M, Playan E, Abbasi F, Navabian M, Lattore B (2013b) Optimum design of alternate and conventional furrow fertigation to minimize nitrate loss. J Irrig Drain Eng 139(11):911–921. doi:10.1061/(ASCE)IR.1943-4774.0000635

Ebrahimian H, Keshavarz MR, Playán E (2014) Surface fertigation: a review, gaps and needs. Span J Agric Res 12(3):820–837

Feddes A, Kowalik PJ, Zaradny H (1978) Simulation of field water use and crop yield. Wiley, New York

Gärdenäs A, Hopmans JW, Hanson BR, Šimůnek J (2005) Two-dimensional modeling of nitrate leaching for various fertigation scenarios under micro-irrigation. Agric Water Manag 74:219–242

Hanson BR, Šimůnek J, Hopmans JW (2006) Numerical modeling of urea-ammonium-nitrate fertigation under microirrigation. Agric Water Manag 86:102–113

Hou Z, Li P, Li B, Gong J, Wang Y (2007) Effects of fertigation scheme on N uptake and N use efficiency in cotton. Plant Soil 290:115–126

Lazarovitch N, Warrick AW, Furman A, Zerihun D (2009) Subsurface water distribution from furrows described by moment analyses. J Irrig Drain Eng 135(1):7–12

Mailhol JC, Crevoisier D, Triki K (2007) Impact of water application conditions on nitrogen leaching under furrow irrigation: experimental and modeling approaches. Agric Water Manag 87(3):275–284

Playán E, Faci JM (1997) Border fertigation: field experiments and a simple model. Irrig Sci 17(4):163–171

Rocha D, Abbasi F, Feyen J (2006) Sensitivity analysis of soil hydraulic properties on subsurface water flow in furrows. J Irrig Drain Eng 132(4):418–424

Sabillón GN, Merkley GP (2004) Fertigation guidelines for furrow irrigation. Span J Agric Res 2(4):576–587

Šimůnek J, Hopmans JW (2009) Modeling compensated root water and nutrient uptake. Ecol Model 220(4):505–521. doi:10.1016/j.ecolmodel.11.004

Šimůnek J, van Genuchten MT, Šejna M (2008) Development and applications of the HYDRUS and STANMOD software packages and related codes. Vadose Zone J 7(2):587–600. doi:10.2136/VZJ2007.0077

Siyal AA, Bristow KL, Šimůnek J (2012) Minimizing nitrogen leaching from furrow irrigation through novel fertilizer placement and soil management strategies. Agric Water Manag 115:242–251

Soroush F, Mostafazadeh-Fard B, Mousavi SF, Abbasi F (2012) Solute distribution uniformity and fertilizer losses under meandering and standard furrow irrigation methods. Aust J Crop Sci 6(5):884–890

Vrugt JA, Hopmans JW, Šimůnek J (2001) Calibration of a two-dimensional root water uptake model. Soil Sci Soc Am J 65(4):1027–1037

Vrugt JA, Van Wijk MT, Hopmans JW, Šimůnek J (2002) One-, two-, and three-dimensional root water uptake functions for transient modeling. Water Resour Res 37(10):2457–2470

Warrick AW, Lazarovitch N, Furman A, Zerihun D (2007) Explicit infiltration function for furrows. J Irrig Drain Eng 133(4):307–313

Wöhling T, Mailhol JC (2007) A physically based coupled model for simulating 1D surface—2D subsurface flow and plant water uptake in irrigation furrows. II: model test and evaluation. J Irrig Drain Eng 133(6):548–558

Wöhling T, Schmitz GH (2007) A physically based coupled model for simulating 1D surface—2D subsurface flow and plant water uptake in irrigation furrows. I: model development. J Irrig Drain Eng 133(6):538–547

Wöhling Th, Schmitz GH, Mailhol JC (2004a) Modeling two-dimensional infiltration from irrigation furrows. J Irrig Drain Eng 130(4):296–303

Wöhling T, Singh R, Schmitz GH (2004b) Physically based modeling of interacting surface–subsurface flow during furrow irrigation advance. J Irrig Drain Eng 130(5):349–356

Wöhling T, Fröhner A, Schmitz GH, Liedl R (2006) Efficient solution of the coupled one-dimensional surface—two-dimensional subsurface flow during furrow irrigation advance. J Irrig Drain Eng 132(4):380–388

Zerihun D, Sanchez CA, Lazarovitch N, Warrick AW, Clemmens AJ, Bautista E (2014) Modeling flow and solute transport in irrigation furrows. Irrig Drain Syst Eng 3(2):16. doi:10.4172/2168-9768.1000124